[7] S. Semenov, "Modified maximal ratio combining HARQ scheme for HSDPA," in *Proc. IEEE Int. Symp. Personal, Indoor, Mobile Radio Commun. (PIMRC)*, Barcelona, Spain, Sep. 2004, vol. 4, pp. 2451–2453.
[8] E. W. Jang, J. Lee, H.-L. Lou, and J. M. Cioffi, "On the combining schemes for MIMO systems with hybrid ARQ," *IEEE Trans. Wireless Commun.*, vol. 8, no. 2, pp. 836–842, Feb. 2009.
[9] A. Goldsmith, *Wireless Communications*. New York: Cambridge Univ. Press, 2005.
[10] *Draft IEEE 802.16m Evaluation Methodology Document*, IEEE C802. 16m-07/080r3, 2007 [Online]. Available: http://ieee802.org/16
[11] J. N. Laneman, D. N. C. Tse, and G. W. Wornell, "Cooperative diversity in wireless networks: Efficient protocols and outage behavior," *IEEE Trans. Inf. Theory*, vol. 50, no. 12, pp. 3062–3080, Dec. 2004.
[12] H. Long, K. Zheng, W. Wang, and F. Wang, "Approximate performance analysis of the incremental relaying protocol and modification," in *Proc. IEEE Veh. Technol. Conf. (VTC) 2009 Fall*, Anchorage, AK, Sep. 2009, pp. 1–5.
[13] J. Gu, Y. Zhang, and D. C. Yang, "Modeling conditional FER for hybrid ARQ," *IEEE Commun. Lett.*, vol. 10, no. 5, pp. 384–386, May 2006.
[14] H. Long, W. Wang, K. Zheng, and F. Wang, "Performance analysis on conditional error ratio in HARQ transmission," in *Proc. IEEE Int. Symp. Microw., Antenna, Propag. EMC Technol. for Wireless Commun. (MAPE)*, Beijing, China, Oct. 2009, pp. 304–309.

Cooperative Multiband Joint Detection With Correlated Spectral Occupancy in Cognitive Radio Networks

Khalid Hossain, Benoît Champagne, and Ayman Assra

***Abstract*—In this paper, a frequency-coupled optimum linear energy combiner (OLEC) structure, recently proposed for single user scenarios, is generalized to multiple users and integrated into the spatial-spectral joint detection framework introduced by Quan *et al.*, to take further advantage of subband occupancy correlation in cooperative wideband spectrum sensing. In particular, the design of the detection thresholds and fusion weights used by a bank of subband multiuser OLECs is formulated as a joint optimization problem, i.e. maximization of aggregate opportunistic throughput under interference constraints (or vice versa). Through numerical experiments with a Markov model of subband occupancy, the proposed scheme is shown to significantly enhance CR network performance in terms of these global metrics.**

***Index Terms*—Cognitive radio, cooperative processing, multiband joint detection, spectrum sensing.**

I. Introduction

Cognitive radios (CRs), which maintain awareness of their environment through spectrum sensing, have emerged as a key enabling technology for dynamic spectrum access [1], [2]. Specifically, CRs must have the capability to detect and opportunistically use momentarily silent portions of the licensed frequency spectrum, called *spectrum holes* [3]. In this scenario, one refers to a user of the wireless system to which the frequency band has been licensed (e.g., WLAN or broadcast television) as a primary user (PU), and to the CR of interest as a secondary user (SU). Spectrum sensing has gained further importance as CR is an integral component of the IEEE 802.22 standard and the focus of other emerging applications [4]. In practice, spectrum sensing must be fast and accurate in order to maximize the opportunistic throughput without adding unacceptable level of interference to the PUs. Until now, several approaches have been considered for this application, including matched filtering, cyclo-stationary feature extraction, and energy detection [2]. The extension of spectrum sensing techniques to multiple antenna CR is considered in [5], [6].

Many studies, such as [7] and [8], advocate the use of energy detection for spectrum sensing since it can meet the basic requirements of CR systems while offering flexibility and robustness in implementation. In this approach, the energy of the received signal is computed and used in a binary hypothesis test to decide the occupancy state of the frequency band under probing [9]. Energy detection can be applied in both narrowband and wideband settings, where in the latter case, it is usually performed by dividing the wideband spectrum into smaller component subbands and carrying out narrowband detection in each subband independently [10]. Recently, *joint* multiband energy detection, where the thresholds used in individual subbands are determined from wideband considerations, has shown great promises for spectrum sensing in CR networks [11]. In this scheme, the cost of interfering with the PUs and the Shannon theoretic capacity for each subband are applied to define global measures of *aggregate interference* and *aggregate opportunistic throughput*, respectively. Subsequently, an optimum set of detection thresholds is designed that maximizes the opportunistic throughput aggregated over all the subbands while keeping the aggregate interference under a critical value.

Alongside these developments, compromised detection due to multipath fading and shadowing has oriented research efforts towards *cooperative* spectrum sensing. In this formulation, sensing information from multiple CRs experiencing different channel conditions is combined at a fusion center to provide more reliable detection of the PU signals by exploiting the built-in spatial diversity of the CR network [12], [13]. The extension of joint multiband energy detection to cooperative spectrum sensing is considered in [11], where further performance enhancements are demonstrated. In [14], cooperative spectrum sensing is performed using channel gain (CG) maps, which enable tracking the location and transmit powers of multiple PUs. In [15], the effect of time dispersive reporting channels on cooperative spectrum sensing is investigated, where the authors propose a widely linear fusion scheme to exploit the multipath nature of the reporting channels.

Existing approaches for wideband spectrum sensing employ a decoupled processing structure in which hypothesis-testing in any given subband is carried out on the energy computed from the observed data in that particular subband only, i.e., independently of other subbands' data. This is so even for the joint multiband energy detection schemes in [11], where only the detection thresholds used in individual subbands are optimized from a wideband perspective. While the frequency-decoupled structure is optimal when the occupancies of the frequency subbands are independent of each other, this condition is generally not satisfied, especially in the presence of wideband PU signals, such as broadcast television or WLAN systems [16]. As a result, more recently, the topic of spectrum sensing in the presence of correlation between the frequency subband occupancies has been gaining notable attention [17], [18]. To exploit such correlation and thus improve sensing performance, [19] proposes a novel (noncooperative) detector structure

Manuscript received July 21, 2011; revised December 01, 2011; accepted January 22, 2012. Date of publication February 13, 2012; date of current version April 13, 2012. The associate editor coordinating the review of this manuscript and approving it for publication was Prof. Amir Leshem. This work was supported by InterDigital Canada Ltée., the Natural Sciences and Engineering Research Council of Canada, and the Government of Québec under the PROMPT program.

The authors are with the Department of Electrical and Computer Engineering, McGill University, Montréal, QC H3A 2A7, Canada (e-mail: benoit.champagne@mcgill.ca).

Color versions of one or more of the figures in this paper are available online at http://ieeexplore.ieee.org.

Digital Object Identifier 10.1109/TSP.2012.2187521

in which energy measurements from multiple subbands are linearly combined, using weights derived from a minimum mean-square error (MMSE) criterion, to form a summary statistic for binary detection in a given subband. This frequency-coupled detector structure, referred to as the optimum linear energy combiner (OLEC), is shown to significantly outperform the traditional frequency-decoupled detector.

In this paper, we extend and integrate the OLEC detector [19] into the spatial-spectral joint detection framework of [11], in order to further exploit *a priori* knowledge of subband occupancy correlation in cooperative wideband spectrum sensing. We first propose a multiuser extension of the OLEC in which the energy measurements from cooperating CRs are linearly weighted at the fusion center, prior to applying optimum linear MMSE combining across the frequency dimension. We analyze the performance of the new multiuser OLEC and derive closed-form expressions for its probabilities of false alarm and missed detection. Using these expressions, we then formulate the joint optimization problem for the set of detection thresholds and fusion weights used by a bank of subband multiuser OLECs, with the aim to maximize the (wideband) aggregate opportunistic throughput under aggregate interference constraints.[1] Through numerical experiments, we demonstrate that the application of the multiuser OLEC in cooperative wideband frameworks can significantly enhance the performance of spatial-spectral joint detection in terms of these global metrics, when compared to the original decoupled multiband processing structure in [11].

The paper is organized as follows. The multiuser wideband system model under consideration for CR networks is exposed in Section II. In Section III, we extend the OLEC detector structure to the cooperative scenario and analyze its performance. In Section IV, we formulate the joint optimization problem for the detection thresholds and fusion weights in this extended structure. In Section V, we present simulation results of various detection scenarios and finally, Section VI concludes the paper.

II. Problem Formulation

We consider a scenario in which N spatially distributed SUs, indexed by $\nu \in \{0,1,\ldots,N-1\}$, collaborate to detect the presence of one or more PU signals over a given wideband frequency range.[2] Assuming a frame-based K-point discrete Fourier transform (DFT) operation, the mth sample of the signal observed by the νth SU in the kth subband can be expressed as (see, e.g. [20]):

$$R_{\nu,k}(m) = H_{\nu,k} S_k(m) + V_{\nu,k}(m) \tag{1}$$

where $k \in \{0,1,\ldots,K-1\}$ is the frequency index, $m \in \{0,1,\ldots,M-1\}$ is the frame index, and M is the total number of available frames for detection. In (1), $S_k(m)$, $H_{\nu,k}$, and $V_{\nu,k}(m)$ respectively denote: the PU signal component in the kth frequency subband at time m; the channel response between the transmitter of this PU signal and the νth SU; and the additive receiver noise. The ordered sets of PU signal samples and SU background noise samples, i.e., $\{S_k(m)\}$ and $\{V_{\nu,k}(m)\}_{\nu=0}^{N-1}$, are modeled as $N+1$ independent random processes, whereby, for any given state of occupancy of the wideband channel, samples from each process are independent across frequency and frame indices, and obey a zero-mean complex circular Gaussian distribution. The noise variance, $\sigma_{\nu,k}^2 \triangleq E[|V_{\nu,k}(m)|^2]$, and the channel squared magnitude response, $G_{\nu,k} \triangleq |H_{\nu,k}|^2$, are assumed to be known from *a priori* estimation and to remain approximately constant during the processing interval.[3] In the absence of a PU signal in subband k (hypothesis $\mathcal{H}_{0,k}$), we set $E[|S_k(m)|^2] = 0$, while in the presence of a PU signal in subband k (hypothesis $\mathcal{H}_{1,k}$), we set $E[|S_k(m)|^2] = 1$ without loss of generality. In the former case, (1) reduces in effect to $R_{\nu k}(m) = V_{\nu k}(m)$.

We model the occupancy of the kth subband by means of a binary (indicator) random variable, B_k, with realization $b_k \in \{0,1\}$, where 0 represents a spectrum hole and 1 indicates the presence of a PU in the kth subband, corresponding to hypotheses $\mathcal{H}_{0,k}$ and $\mathcal{H}_{1,k}$, respectively. The multiband spectrum occupancy is represented by means of random vector $\mathbf{B} = [B_0, B_1, \ldots, B_{K-1}]^T$, with realizations $\mathbf{b} = [b_0, b_1, \ldots, b_{K-1}]^T \in \{0,1\}^K$. We define the mean vector $\boldsymbol{\mu} = E[\mathbf{B}]$, with entries $\mu_i = E[B_i] = \Pr(B_i = 1)$, and the correlation matrix $\boldsymbol{\Lambda} = E[\mathbf{B}\mathbf{B}^T]$, with entries $\lambda_{ij} = E[B_i B_j] = \Pr(B_i = B_j = 1)$. Note that the conditional signal power of the PU in the kth subband, given the spectrum occupancy $\mathbf{B} = \mathbf{b}$, may be expressed compactly as $E[|S_k(m)|^2|\mathbf{B} = \mathbf{b}] = b_k$. We assume that random vector $\mathbf{B}$ is independent of the noise processes, $\{V_{\nu k}(m)\}_{\nu=0}^{N-1}$, and remains unchanged during the detection interval.

The collection of energy measurements from the N SUs in the kth subband over the M frames of interest is represented by the following $N \times 1$ vector:

$$\mathbf{Y}_k = \left[Y_{0,k}, Y_{1,k}, \ldots, Y_{(N-1),k}\right]^T, \quad \text{where}$$
$$Y_{\nu,k} = \sum_{m=0}^{M-1} |R_{\nu,k}(m)|^2. \tag{2}$$

Detection is carried out at the so-called fusion centre, which may be one of the cooperating SUs (e.g., the zeroth SU) or a network entity (e.g., a base station). The fusion center makes decisions about the occupancy of the multiple subbands based on the measurements collected from all the SUs over the frequency band of interest, i.e., $\{\mathbf{Y}_k : k = 0,\ldots,K-1\}$. Although a few different fusion schemes have been proposed in the literature for generating test statistics from measurements made at multiple spatially dispersed SUs, here, we consider the linear weighing scheme[4] discussed in [11] and [12]. In this scheme, the summary statistic corresponding to frequency index k is obtained as:

$$U_k = \sum_{\nu=0}^{N-1} w_{\nu,k} Y_{\nu,k} = \mathbf{w}_k^T \mathbf{Y}_k \tag{3}$$

where $\mathbf{w}_k = [w_{0,k}, w_{1,k}, \ldots, w_{(N-1),k}]^T$ is a vector of nonnegative weights, used to combine the energy measurements from the N SUs for the kth subband.

Given such a fusion scheme, our objective is to develop an efficient detector that will enable the SUs (via the fusion center) to determine the wideband PU's spectrum occupancy, which is tantamount to estimating the unknown value of binary vector $\mathbf{B}$. This problem has been considered in [11], where the aim is to jointly design a set of detection thresholds and combiner weights that maximize the opportunistic throughput aggregated over all the subbands, while keeping the aggregate interference under a critical value. However, the resulting scheme employs a decoupled processing structure, which neglects the correlation between subband occupancies. To benefit from *a priori* knowledge of the PU's spectral occupancy, an optimum linear energy combiner (OLEC) for single-user CR was introduced in [19], in which multiband energy measurements are linearly combined based on a MMSE criterion to form a sufficient statistic for binary detection in a given subband. Below, we

[1]Alternatively, it is possible to minimize the aggregate interference under constraint on the aggregate opportunistic throughput.

[2]In this work, no particular assumptions are made regarding the specific nature of the licensed signal: it could be formed by a single wideband PU signal (i.e., TV broadcasting), or multiple PU signals occupying different portions of the spectrum according to a pre-established resource allocation strategy.

[3]Estimation of the channel gains is further discussed in [1], [11].

[4]This choice is motivated by several considerations, including: low computational complexity, mathematically tractable formulation of the design problem, and wide acceptance in the cooperative spectrum sensing literature.

combine both approaches and propose a multiuser generalization of the single-user OLEC detector for applications to *cooperative* wideband spectrum sensing. We proceed in two steps: 1) Extension of the OLEC [19] to multiple users and 2) optimization of the detection thresholds and fusion weights used in the different subbands via the joint multiband approach in [11].

III. The Multiuser OLEC Detector

Let $\mathbf{U} = [U_0, U_1, \dots, U_{K-1}]^T$ denote the random vector of weighted energy measurements (i.e. after data fusion) over the K frequency subbands, and let $\mathbf{u} = [u_0, u_1, \dots, u_{K-1}]^T$ denote its corresponding realization, which is available at the fusion center. Within the above Bayesian framework, the maximum *a posteriori* (MAP) estimator of $\mathbf{B}$, given $\mathbf{U} = \mathbf{u}$, is defined as

$$\hat{\mathbf{B}}_{\text{MAP}} = \arg\max_{\mathbf{b}} L_{\text{MAP}}(\mathbf{b}|\mathbf{u}) \tag{4}$$

where $L_{\text{MAP}}(\mathbf{b}|\mathbf{u})$ is the log-likelihood function of $\mathbf{B}$ given $\mathbf{U} = \mathbf{u}$. Using the modeling assumptions in Section II, $L_{\text{MAP}}(\mathbf{b}|\mathbf{u})$ in (4) can be expressed in the form:

$$L_{\text{MAP}}(\mathbf{b}|\mathbf{u}) = \ln P_{\mathbf{B}}(\mathbf{b}) - \sum_{k=0}^{K-1} \ln f_{U_k|B_k}(u_k|b_k) \tag{5}$$

where $f_{U_k|B_k}(u_k|b_k)$ denotes the conditional probability density function (PDF) of U_k given $B_k = b_k$. This function depends on the system parameters $G_{\nu,k}, \sigma^2_{\nu,k}$ and $w_{\nu,k}$ for $\nu \in \{0, 1, \dots, N-1\}$.

Considering the more realistic situation where the subband occupancies are correlated, the MAP detector does not decouple and leads to a nonlinear integer optimization in K-dimensional space, with high computational complexity of order 2^K. Alternatively, the frequency-coupled OLEC in [19] is designed to exploit correlation between subband occupancies in the *single-user* detection process without the computational cost of the full multiband MAP. Below, we develop a *multiuser* counterpart to the single-user OLEC detector and analyze its performance in terms of detection and false alarm probabilities.

A. The Detector Structure

We seek to detect the kth subband's occupancy, as represented by B_k, through a single hypothesis test on a summary statistics generated by linearly combining the weighted energy measurements available at the fusion center. Consequently, we define $\hat{B}_k$, the estimate of the occupancy of the kth subband, as an affine transformation on the weighted energy vector $\mathbf{U}$:

$$\hat{B}_k = \boldsymbol{\xi}_k^T \mathbf{U} + \epsilon_k = \sum_{i=0}^{K-1} \xi_{k,i} U_i + \epsilon_k. \tag{6}$$

As in the single-user case, the weight vector $\boldsymbol{\xi}_k = [\xi_{k,0}, \xi_{k,1}, \dots, \xi_{k,K-1}]^T$ and the constant ϵ_k are obtained as the minimizer of the mean-square error:

$$J(\boldsymbol{\xi}_k, \epsilon_k) = E\left[(\hat{B}_k - B_k)^2\right] = E\left[\left(\boldsymbol{\xi}_k^T \mathbf{U} + \epsilon_k - B_k\right)^2\right]. \tag{7}$$

By defining the centered quantities $\bar{\mathbf{U}} = \mathbf{U} - E[\mathbf{U}]$ and $\bar{B}_k = B_k - \mu_k$, where $\mu_k = E[B_k]$, the MMSE weight vector can be obtained as

$$\boldsymbol{\xi}_k^o = E[\bar{\mathbf{U}}\bar{\mathbf{U}}^T]^{-1} E[\bar{\mathbf{U}}\bar{B}_k]. \tag{8}$$

Furthermore, since B_k has a nonzero mean, the optimum value of the bias term ϵ_k is nonzero in general and given by $\epsilon_k^o = \mu_k - \boldsymbol{\xi}_k^{oT} E[\mathbf{U}]$. Using (3), the first and second moments needed to compute the MMSE solution $\boldsymbol{\xi}_k^o$ and ϵ_k^o can be expressed in the form:

$$\begin{aligned} E[U_i] = \mathbf{w}_i^T E[\mathbf{Y}_i], \quad E[\bar{U}_i \bar{B}_k] = \mathbf{w}_i^T E[\bar{\mathbf{Y}}_i \bar{B}_k], \\ E[\bar{U}_i \bar{U}_j] = \mathbf{w}_i^T E\left[\bar{\mathbf{Y}}_i \bar{\mathbf{Y}}_j^T\right] \mathbf{w}_j^T \end{aligned} \tag{9}$$

where we define the centered random vector $\bar{\mathbf{Y}}_k = \mathbf{Y}_k - E[\mathbf{Y}_k]$. In turn, by substituting (1) into (2) and making use of the signal model assumptions in Section II, the following expressions can be derived for the various moments appearing on the right-hand sides of the equations in (9):

$$E[Y_{\nu,i}] = M\left(\mu_i G_{\nu,i} + \sigma^2_{\nu,i}\right)$$

$$E[\bar{Y}_{\nu,i} \bar{B}_k] = M(\lambda_{i,k} - \mu_i \mu_k) G_{\nu,i} \tag{10}$$

$$\begin{aligned} E[\bar{Y}_{\nu,i} \bar{Y}_{\eta,j}] = M^2(\lambda_{i,j} - \mu_i \mu_j) G_{\nu,i} G_{\eta,j} + M(\mu_i G_{\nu,i} G_{\eta,i} \\ + 2\mu_i G_{\nu,i} \sigma^2_{\nu,i} \delta_{\nu,\eta} + \sigma^4_{\nu,i} \delta_{\nu,\eta}) \delta_{i,j} \end{aligned} \tag{11}$$

where we recall that $\lambda_{i,j} = E[B_i B_j]$ and $\delta_{i,j} = 1$ if $i = j$, 0 otherwise. Details surrounding the mathematical derivation of these moments can be found in [21]. Finally, the multiuser OLEC based detector for the kth subband can be formulated as

$$Z_k = \boldsymbol{\xi}_k^{oT} \mathbf{U} \underset{\mathcal{H}_{0,k}}{\overset{\mathcal{H}_{1,k}}{\gtrless}} \gamma_k. \tag{12}$$

It should be noted that, for convenience, the bias term ϵ_k^o is absorbed in the detection threshold γ_k, and $\boldsymbol{\xi}_k^o$ can be normalized such that $\xi_{kk}^o = 1$. In essence, the multiuser OLEC detector employs the wideband multiuser information available at the fusion center, represented by the vector $\mathbf{U}$ of spatially weighted energy measurements U_i (3) for *all* frequency subbands $i \in \{0, 1, \dots, K-1\}$, to make an informed decision about the state of occupancy B_k of the kth subband. To this end, the computation of the linear combiner weight vector $\boldsymbol{\xi}_k$ optimally exploits (in the MMSE sense) the *a priori* knowledge about the state of occupancy of the multiple subbands comprising the wide frequency band of interest, specifically the first and second moments of the occupancy vector $\mathbf{B}$, i.e. μ_i and $\lambda_{i,j}$, respectively.

B. Performance Metrics

The minimum attainable probability of missed detection for a given upper limit on the probability of false alarm provides an objective measure of the detection performance. Hence, we compute these probabilities for the multiuser OLEC detector developed here. Conditioned on $B_k = b_k$, the mean and variance of the test statistic, Z_k, in (12) can be written as

$$\begin{aligned} E[Z_k|B_k = b_k] = \boldsymbol{\xi}_k^{oT} E[\mathbf{U}|B_k = b_k], \\ \text{Var}[Z_k|B_k = b_k] = \boldsymbol{\xi}_k^{oT} E[\bar{\mathbf{U}}\bar{\mathbf{U}}^T|B_k = b_k] \boldsymbol{\xi}_k^o. \end{aligned} \tag{13}$$

Using the definition of U_k in (3), we can show

$$\begin{aligned} E[U_i|B_k = b_k] = \mathbf{w}_i^T E[\mathbf{Y}_i|B_k = b_k], \\ E[\bar{U}_i \bar{U}_j|B_k = b_k] = \mathbf{w}_i^T E\left[\bar{\mathbf{Y}}_i \bar{\mathbf{Y}}_j^T|B_k = b_k\right] \mathbf{w}_j^T. \end{aligned} \tag{14}$$

The evaluation of the expected values of the right-hand sides of the equations in (14) yields

$$\begin{aligned} E[Y_{\nu,i}|B_k = b_k] = M\left(G_{\nu,i} \mu_{i|k} + \sigma^2_{\nu,i}\right), \\ E[\bar{Y}_{\nu,i} \bar{Y}_{\eta,j}|B_k = b_k] = M^2 G_{\nu,i} G_{\eta,j} (\lambda_{i,j|k} - \mu_{i|k} \mu_{j|k}) \\ + M\left[\mu_{i|k} G_{\nu,i} G_{\eta,j} + 2\mu_{i|k} G_{\nu,i} \sigma^2_{\nu,i} \delta_{\nu,\eta} \right. \\ \left. + \sigma^4_{\nu,i} \delta_{\nu,\eta}\right] \delta_{i,j} \end{aligned} \tag{15}$$

where, for convenience, we have introduced the short-hand notations $\mu_{i|k} \equiv E[B_i|B_k = b_k]$ and $\lambda_{i,j|k} \equiv E[B_i B_j|B_k = b_k]$. According to the central limit theorem, for a sufficiently large M, the random variables $Y_{\nu,k}$ in (2) and, in turn, U_k in (3) and Z_k in (12) can be assumed to be normally distributed under both $\mathcal{H}_{0,k}$ and $\mathcal{H}_{1,k}$. Consequently, the probabilities of false alarm and missed detection associated with the multiuser OLEC detector are given by

$$\begin{aligned} P_f^{(k)}(\mathbf{W}, \gamma_k) &= Q\left(\frac{\gamma_k - E[Z_k|B_k = 0]}{\sqrt{\mathrm{Var}[Z_k|B_k = 0]}}\right) \\ P_m^{(k)}(\mathbf{W}, \gamma_k) &= 1 - Q\left(\frac{\gamma_k - E[Z_k|B_k = 1]}{\sqrt{\mathrm{Var}[Z_k|B_k = 1]}}\right) \end{aligned} \tag{16}$$

where we define $Q(x) = \left(\frac{1}{\sqrt{2\pi}}\right) \int_x^\infty e^{\frac{t^2}{2}} dt$. These performance metrics depend on the specific choice of weights used to combine the energy measurements from the SUs, as represented over the frequency band of interest by matrix $\mathbf{W} = [\mathbf{w}_0, \mathbf{w}_1, \ldots, \mathbf{w}_{K-1}]$.

IV. Cooperative Multiband Joint Detection

Single-user detection schemes are susceptible to blockage effects, such as shadowing or multipath fading, that negatively impact the sensing performance. Current literature advocates the use of multiuser collaboration among spatially distributed CR terminals in order to overcome these effects. Here, we further extend and integrate the multiuser OLEC detector into the joint spatial-spectral detection framework of [11] for optimum cooperative wideband spectrum sensing in the presence of subband occupancy correlation.

A. Spatial-Spectral Joint Detection

We consider a multiuser, multiband joint detection framework where we seek the optimum use of the unoccupied spectrum without introducing undesirable levels of interference to the PUs. To this aim, we quantify the spectrum utilization by the SUs and the resulting interference to the PU using two global (i.e., wideband) performance metrics, as originally proposed in [11]. Using (12) and (16), we first define the following vectors: $\boldsymbol{\gamma} = [\gamma_0, \gamma_1, \ldots, \gamma_{K-1}]^T$, $\mathbf{P}_f(\mathbf{W}, \boldsymbol{\gamma}) = [P_f^{(0)}(\mathbf{W}, \gamma_0), \ldots, P_f^{(K-1)}(\mathbf{W}, \gamma_{K-1})]^T$, and $\mathbf{P}_m(\mathbf{W}, \boldsymbol{\gamma}) = [P_m^{(0)}(\mathbf{W}, \gamma_0), \ldots, P_m^{(K-1)}(\mathbf{W}, \gamma_{K-1})]^T$, where the dependence on the weight matrix $\mathbf{W}$ has been made explicit. Using these notations, the *aggregate opportunistic throughput* available to the SUs and the *aggregate interference* to the PUs can be defined for the multiuser case as follows, respectively:

$$R(\mathbf{W}, \boldsymbol{\gamma}) \triangleq \boldsymbol{r}^T [\mathbf{1} - \boldsymbol{P}_f(\mathbf{W}, \boldsymbol{\gamma})], \; C(\mathbf{W}, \boldsymbol{\gamma}) \triangleq \boldsymbol{c}^T \boldsymbol{P}_m(\mathbf{W}, \boldsymbol{\gamma}). \tag{17}$$

In (17), vector $\boldsymbol{r} = [r_0, r_1, \ldots, r_{K-1}]^T$, where $r_k \geq 0$ represents the throughput achievable over the kth subband by the SUs. The value of r_k can be determined from experimental measurements in a given radio environment or, otherwise, estimated using Shannon theoretic capacity formula [22]. Also, vector $\boldsymbol{c} = [c_0, c_1, \ldots, c_{K-1}]^T$, where $c_k \geq 0$ represents the cost of interfering with the PU in the kth subband.

Given these performance metrics, we seek a jointly optimum set of detection thresholds, $\boldsymbol{\gamma}$, and fusion weights, $\mathbf{W}$, that achieves one of the following: 1) maximizes the aggregate opportunistic throughput given an upper bound, $\epsilon > 0$, on the aggregate interference or 2) minimizes the aggregate interference given a lower bound, $\delta > 0$, on the aggregate opportunistic throughput. Furthermore, to limit the interference and achieve a minimum opportunistic utilization in each subband, we impose the constraints: $P_m^{(k)}(\mathbf{W}, \gamma_k) \leq \alpha_k$ and $P_f^{(k)}(\mathbf{W}, \gamma_k) \leq \beta_k$ for $k = 0, 1, \ldots, K-1$, where it is realistic to assume $0 \leq \alpha_k \leq \frac{1}{2}$ and $0 \leq \beta_k \leq \frac{1}{2}$. Using (16) and the fact that the function $Q(x)$ is monotonically decreasing, the above constraints on $P_m^{(k)}(\mathbf{W}, \gamma_k)$ and $P_f^{(k)}(\mathbf{W}, \gamma_k)$ can be transformed into the following linear constraints on the feasible set of the threshold vector $\boldsymbol{\gamma}$: $\gamma_{\min,k} \leq \gamma_k \leq \gamma_{\max,k}$, where $\gamma_{\min,k} \triangleq E[Z_k|B_k = 0] + Q^{-1}(\beta_k)\sqrt{\mathrm{Var}[Z_k|B_k = 0]}$, $\gamma_{\max,k} \triangleq E[Z_k|B_k = 1] + Q^{-1}(1 - \alpha_k)\sqrt{\mathrm{Var}[Z_k|B_k = 1]}$, and the expressions for the conditional mean and variance of Z_k are available from Section III-B. The joint spatial-spectral optimization problems for $\boldsymbol{\gamma}$ and $\mathbf{W}$ can therefore be formulated as follows.

- Maximization of aggregate opportunistic throughput with constraint on aggregate interference:

$$\max_{\boldsymbol{\gamma}, \mathbf{W}} \; R(\mathbf{W}, \boldsymbol{\gamma}) \text{ s.t. } C(\mathbf{W}, \boldsymbol{\gamma}) \leq \epsilon, \; \gamma_{\min,k} \leq \gamma_k \leq \gamma_{\max,k}. \tag{18}$$

- Minimization of aggregate interference with constraint on aggregate opportunistic throughput:

$$\min_{\boldsymbol{\gamma}, \mathbf{W}} \; C(\mathbf{W}, \boldsymbol{\gamma}) \text{ s.t. } R(\mathbf{W}, \boldsymbol{\gamma}) \geq \delta, \; \gamma_{\min,k} \leq \gamma_k \leq \gamma_{\max,k}. \tag{19}$$

Solving these problems numerically is challenging since the expressions for $P_f^{(k)}(\mathbf{W}, \gamma_k)$ and $P_m^{(k)}(\mathbf{W}, \gamma_k)$ in (16) are neither convex nor concave functions in the search variables $\boldsymbol{\gamma}$ and $\mathbf{W}$. In [11], two different approaches are proposed to overcome a similar difficulty in the case of uncorrelated subband occupancy: a bounding approach and a sequential approach. The former cannot be readily extended to the framework under consideration here, i.e., coupled frequency detector with correlated subband occupancy, due to the dependence of each MMSE linear combiner $\boldsymbol{\xi}_k^o$ (8) on the complete fusion weight matrix $\mathbf{W}$. However, the sequential approach can be extended to the new framework, and this is further discussed below.

B. Sequential Approach

In [11], a two-step sequential optimization procedure is described, which can provide a good approximation to the optimal solution of the original problem, but with much reduced complexity. The two steps are as follows.

1) *Spatial optimization*: The weight coefficients in each subband are chosen to maximize a chosen performance measure for signal detection.
2) *Spectral optimization*: For the given optimal choice of weights, the threshold vector $\boldsymbol{\gamma}$ is chosen to maximize the aggregate opportunistic throughput under interference constraint (or minimize aggregate interference under a throughput constraint).

This same method is adopted in our work. In the spatial optimization step, we consider the *modified signal deflection* of U_k as a performance measure for signal detection within the kth subband:

$$d_k^2(\mathbf{w}_k) \triangleq \frac{(E[U_k|B_k = 1] - E[U_k|B_k = 0])^2}{\mathrm{Var}[U_k|B_k = 1]}. \tag{20}$$

In effect, this quantity can be viewed as a measure of the signal-to-noise ratio (SNR) available for the purpose of detection based on U_k. Using the expressions in (14) for the conditional moments of U_k, $d_k^2(\mathbf{w}_k)$ can be expressed in terms of $\mathbf{w}_k$ as follows:

$$d_k^2(\mathbf{w}_k) = \frac{\left(M \mathbf{w}_k^T \mathbf{G}_k\right)^2}{\mathbf{w}_k^T \boldsymbol{\Sigma}_{k|1} \mathbf{w}_k} \tag{21}$$

where $\boldsymbol{G}_k = [G_{0,k}, G_{1,k}, \ldots, G_{(N-1),k}]^T$ is the vector of the channel squared magnitude responses between the PU and the N collaborating SUs in the kth subband, and matrix $\boldsymbol{\Sigma}_{k|1} = E[\bar{\mathbf{Y}}_k \bar{\mathbf{Y}}_k^T | B_k = 1]$, whose entries can be computed based on (15). Our aim is to chose the weight vector $\mathbf{w}_k$ that maximizes $d_k^2(\mathbf{w}_k)$ for each subband. Since $d_k^2(\mathbf{w}_k)$ is invariant under scaling of $\mathbf{w}_k$, we must impose the additional constraint $\|\mathbf{w}_k\|_2 = 1$ to obtain a unique solution, where $\|.\|_2$ denotes the Euclidean norm of its vector argument. The optimal fusion weight vector for the kth subband is finally obtained in the form

$$\mathbf{w}_k^o = \frac{\mathbf{\Sigma}_{k|1}^{-1}\mathbf{G}_k}{\left\|\mathbf{\Sigma}_{k|1}^{-1}\mathbf{G}_k\right\|_2}. \tag{22}$$

In the spectral optimization step, we fix the fusion weight matrix $\mathbf{W}$ to its optimal value obtained in the previous step, i.e., $\mathbf{W}^o = [\mathbf{w}_0^o, \mathbf{w}_1^o, \ldots, \mathbf{w}_{K-1}^o]$, and seek to find an optimum set of thresholds $\boldsymbol{\gamma}$ across all subbands, by solving the following simplified problems.

- Maximization of aggregate opportunistic throughput under interference constraint:

$$\max_{\boldsymbol{\gamma}} \; R(\mathbf{W}^o, \boldsymbol{\gamma}) \text{ s.t. } C(\mathbf{W}^o, \boldsymbol{\gamma}) \leq \epsilon, \; \gamma_{\min,k} \leq \gamma_k \leq \gamma_{\max,k}. \tag{23}$$

- Minimization of aggregate interference under throughput constraint:

$$\min_{\boldsymbol{\gamma}} \; C(\mathbf{W}^o, \boldsymbol{\gamma}) \text{ s.t. } R(\mathbf{W}^o, \boldsymbol{\gamma}) \geq \delta, \; \gamma_{\min,k} \leq \gamma_k \leq \gamma_{\max,k}. \tag{24}$$

Restricting the parameters α_k and β_k to the interval $[0, \frac{1}{2}]$ ensures that these optimization problems are convex, making it possible to efficiently solve for the global optimum.

V. Numerical Results

In this section, numerical results are presented to evaluate the performance of the proposed OLEC-based cooperative wideband spectrum sensing scheme. We consider a CR network of $N = 2$ spatially distributed SUs, each of which senses a targeted frequency spectrum of 48 MHz bandwidth. The spectrum is equally divided into $K = 8$ subbands, where for each subband, the maximum probabilities of missed detection and false alarm are set to $\alpha_k = 0.2$ and $\beta_k = 0.5$, respectively. We model the correlation between subband occupancies using a homogeneous Markov chain defined over the discrete frequency index k. The initial occupancy state of the chain, B_0, is set to 1 with probability $P_{B_0}(1) = 0.5$, while the occupancy states at frequencies $k = 1, \ldots, K-1$ are generated by means of a binary symmetric transition model with parameter p denoting the probability of a change in occupancy, that is, $P_{B_{k+1}|B_k}(1|0) = P_{B_{k+1}|B_k}(0|1) = p$. Given this model, the moments μ_i, $\mu_{i|k}$, $\lambda_{i,j}$ and $\lambda_{i,j|k}$ introduced in Section II and Section III can be derived analytically, and subsequently $P_f^{(k)}(\mathbf{W}, \gamma_k)$ and $P_m^{(k)}(\mathbf{W}, \gamma_k)$ can be computed exactly from the corresponding expressions in (16). The wireless links between each one of the SU and the PU experience frequency-selective fading. The power delay profiles of the links and other system parameters (i.e., gains $G_{\nu,k}$, throughputs r_k and costs c_k) are taken from [11, Example 2]. Unless indicated differently, it is assumed that $\sigma_{\nu,k}^2 = 1$, $M = 100$ and the correlation between neighboring subband occupancies, $\rho = 1 - 2p = 0.7$.

The numerical results presented below are produced by solving the inequality-constrained convex optimization problems (23) and (24) and then running Monte Carlo simulations of the optimized OLEC-based detector in order to estimate the aggregate measures of performance. Efficient numerical search algorithms such as the interior-point method can be used to find the optimum solution. In our work, we use the Matlab routine `fmincon`, which provides implementations of several constrained minimization algorithms [23].

Fig. 1 plots the maximum aggregate opportunistic throughput achievable by the SUs against the constraint ϵ on the aggregate interference to the PU. By exploiting *apriori* knowledge of the correlation between subband occupancies, the frequency-coupled OLEC detector ($Z_k = {\boldsymbol{\xi}_k^o}^T \mathbf{U}$) results in significant throughput enhancement over the traditional frequency-decoupled scheme ($Z_k = U_k$) in the spatial-spectral joint multiband detection process, and this over a wide range of interference constraints. The same argument is extended to the optimization problem in (24), where the SUs target a specific aggregate opportunistic throughput with minimal attainable aggregate interference. It can be shown as well that the use of the OLEC in multiband joint detection significantly reduces the interference level imposed on the PU.

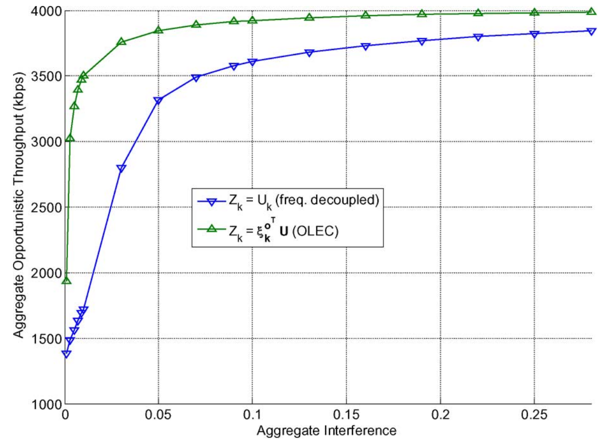

Fig. 1. Maximum aggregate opportunistic throughput for 2-SU CR network against the constraint on aggregate interference to the PU.

Fig. 2(a) plots the maximum aggregate opportunistic throughput as a function of the correlation coefficient between subband occupancies, ρ, under an upper bound on the aggregate interference of $\epsilon = 0.03$. The results show that the OLEC-based joint detection improves the spectrum utilization significantly in the region of highly correlated subband occupancy. In Fig. 2(b), the aggregate opportunistic throughput is plotted against the number of frames available for detection M with an interference upper bound of 0.03. We notice that the use of the frequency-coupled OLEC structure in the multiband joint detection framework enables the multiuser CR networks to maintain higher aggregate throughput in short sensing time scenarios, compared to networks using frequency-decoupled detectors.

Finally, Fig. 3 presents the regions of achievable throughput-interference operation points for different number of SUs. The channels between the SUs and the PU are assumed to be frequency-selective fading with different numbers of resolvable paths: $L_1 = 4$, $L_2 = 6$, $L_3 = 4$, and $L_4 = 6$. The delays of the resolvable paths are selected in a range from 0 to 210 ns, and the corresponding average power gains have values between -1 and -25 dB. It is shown that by utilizing the built-in spatial diversity of the cooperative CR network in the decision-making process on subband occupancy, the maximum aggregate opportunistic throughput increases significantly with the number of SUs, especially in the regions of low interference.

VI. Conclusion

In this paper, we have presented a spatial-spectral joint detector based on the multiuser OLEC for cooperative wideband spectrum sensing in CR networks. The proposed scheme, which employs a frequency-coupled processing structure, has the advantage of exploiting *a priori* knowledge of subband occupancy correlation in making its sensing decisions across a wide frequency band. We formulated the joint optimization problem for the set of detection thresholds and fusion weights used by a bank of subband multiuser OLECs and considered its sequential solution with reduced complexity. Through numerical experiments, we showed that the incorporation of the frequency-coupled OLEC in the spatial-spectral joint detection framework for cooperative wideband spectrum sensing can significantly

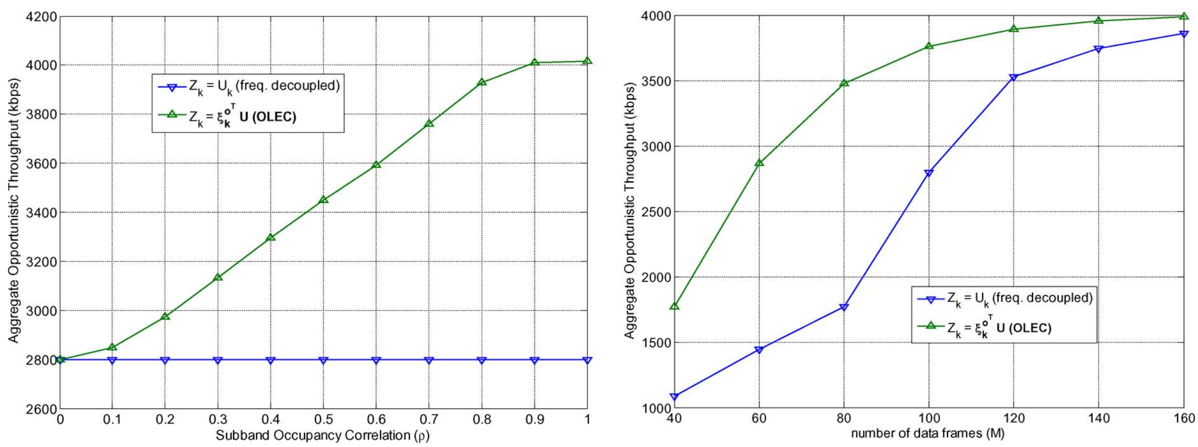

Fig. 2. Maximum aggregate opportunistic throughput for a 2-SU CR network under interference constraint of $\epsilon = 0.03$: (a) versus ρ and (b) versus M.

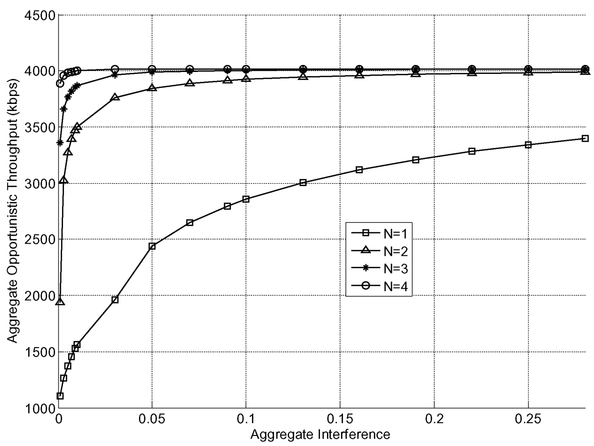

Fig. 3. Achievable throughput-interference regions of the proposed scheme for different number of SUs.

enhance the performance of high data-rate CR networks. Our work has focused on the use of a linear combiner for fusing the narrow-band energy measurements available from the multiple SUs across the band of interest, primarily because of its simplicity and widespread use. Clearly, other possible fusion schemes can be contemplated as well, e.g. involving nonlinear mapping of these energies or derived from optimization of a global criterion. In this context, the choice of an optimal energy fusion scheme remains an interesting avenue for research.

REFERENCES

[1] S. Haykin, "Cognitive radio: Brain-empowered wireless communications," *IEEE J. Sel. Areas Commun.*, vol. 23, no. 2, pp. 201–220, Feb. 2005.

[2] Y.-C. Liang, K.-C. Chen, G. Y. Li, and P. Mahonen, "Cognitive radio networking and communications: An overview," *IEEE Trans. Veh. Technol.*, vol. 60, no. 7, pp. 3386–3407, Sep. 2011.

[3] T. Yücek and H. Arslan, "A survey of spectrum sensing algorithms for cognitive radio applications," *IEEE Commun. Surveys Tuts.*, vol. 11, no. 1, pp. 116–130, Mar. 2009.

[4] J. Wang, M. Ghosh, and K. Challapali, "Emerging cognitive radio applications: A survey," *IEEE Commun. Mag.*, vol. 49, no. 3, pp. 74–81, 2011.

[5] P. Wang, J. Fang, N. Han, and H. Li, "Multiantenna-assisted spectrum sensing for cognitive radio," *IEEE Trans. Veh. Technol.*, vol. 59, no. 4, pp. 1791–1800, May 2010.

[6] D. Ramirez, G. Vazquez-Vilar, R. Lopez-Valcarce, J. Via, and I. Santamaria, "Detection of rank-P signals in cognitive radio networks with uncalibrated multiple antennas," *IEEE Trans. Signal Process.*, vol. 59, no. 8, pp. 3764–3774, Aug. 2011.

[7] Z. Quan, S. Cui, H. V. Poor, and A. H. Sayed, "Collaborative wideband sensing for cognitive radios," *IEEE Signal Process. Mag.*, vol. 25, no. 6, pp. 60–73, Nov. 2008.

[8] S. Atapattu, C. Tellambura, and H. Jiang, "Energy detection based cooperative spectrum sensing in cognitive radio networks," *IEEE Trans. Wireless Commun.*, vol. 10, no. 4, pp. 1232–1241, Apr. 2011.

[9] H. V. Poor, *An Introduction to Signal Detection and Estimation*, 2nd ed. New York: Springer-Verlag, 1994.

[10] A. Taherpour, S. Gazor, and M. Nasiri-Kenari, "Invariant wideband spectrum sensing under unknown variances," *IEEE Trans. Wireless Commun.*, vol. 8, no. 5, pp. 2182–2186, May 2009.

[11] Z. Quan, S. Cui, A. H. Sayed, and H. V. Poor, "Optimal multiband joint detection for spectrum sensing in cognitive radio networks," *IEEE Trans. Signal Process.*, vol. 57, no. 3, pp. 1128–1140, Mar. 2009.

[12] Z. Quan, S. Cui, and A. H. Sayed, "Optimal linear cooperation for spectrum sensing in cognitive radio networks," *IEEE J. Sel. Topics Signal Process.*, vol. 2, no. 1, pp. 28–40, Feb. 2008.

[13] Z. Quan, W.-K. Ma, S. Cui, and A. H. Sayed, "Optimal linear fusion for distributed detection via semidefinite programming," *IEEE Trans. Signal Process.*, vol. 58, no. 4, pp. 2431–2436, Apr. 2010.

[14] S.-J. Kim, E. Dall'Anese, and G. B. Giannakis, "Cooperative spectrum sensing for cognitive radios using Kriged Kalman filtering," *IEEE J. Sel. Topics Signal Process.*, vol. 5, no. 1, pp. 24–36, Feb. 2011.

[15] A. S. Cacciapuoti, M. Caleffi, D. Izzo, and L. Paura, "Cooperative spectrum sensing techniques with temporal dispersive reporting channels," *IEEE Trans. Wireless Commun.*, vol. 10, no. 10, pp. 3392–3402, Oct. 2011.

[16] B.-J. Kang, "Spectrum sensing issues in cognitive radio networks," in *Proc. Int. Symp. Commun. Inf. Technol.*, Jan. 2009, pp. 824–828.

[17] C.-H. Hwang, G.-L. Lai, and S.-C. Chen, "Spectrum sensing in wideband OFDM cognitive radios," *IEEE Trans. Signal Process.*, vol. 58, no. 2, pp. 709–719, Feb. 2010.

[18] H. Li and R. C. Qiu, "A graphical framework for spectrum modeling and decision making in cognitive radio networks," in *Proc. IEEE GLOBECOM Conf.*, Dec. 2010, pp. 1–6.

[19] K. Hossain and B. Champagne, "Wideband spectrum sensing for cognitive radios with correlated subband occupancy," *IEEE Signal Process. Lett.*, vol. 18, no. 1, pp. 35–38, Jan. 2011.

[20] J. C. Park, J. S. Wang, H. G. Kang, S. Yoon, I. Song, and Y. H. Kim, "Detection of variable subband nulling mode for OFDM-based cognitive radio in narrowband interference channels," *IEEE Trans. Wireless Commun.*, vol. 10, no. 3, pp. 782–791, Mar. 2011.

[21] K. S. Hossain, "Wideband spectrum sensing for cognitive radios in the presence of correlation between subband occupancy," M. Eng. thesis, McGill Univ., Montreal, QC, Canada, Aug. 2010.

[22] A. Goldsmith, *Wireless Communications*. Cambridge, U.K.: Cambridge Univ. Press, 2006.

[23] MathWorks, Matlab User's Guide [Online]. Available: http://www.mathworks.com/help/toolbox/optim/ug/fmincon.html